Dynamics of a glass-forming triepoxide studied by dielectric spectroscopy

1999 J. Phys.: Condens. Matter 11 10297

(http://iopscience.iop.org/0953-8984/11/50/322)

J. Phys.: Condens. Matter **11** (1999) 10297–10314. Printed in the UK PII: S0953-8984(99)04671-8

Dynamics of a glass-forming triepoxide studied by dielectric spectroscopy

S Corezzi†, S Capaccioli‡, G Gallone†, M Lucchesi† and P A Rolla†§

† INFM and Department of Physics, University of Pisa, Piazza Torricelli 2, 56126 Pisa, Italy
‡ INFM and Department of Chemical Engineering, Industrial Chemistry and Materials Science, University of Pisa, 56100 Pisa, Italy

E-mail: rolla@mailbox.difi.unipi.it

Received 1 June 1999, in final form 25 August 1999

Abstract. Dielectric measurements of an epoxy resin, N, N-diglycidyl-4-glycidyloxyaniline, have been carried out in the supercooled and glassy phase over a broad frequency range (10^2–6×10^9 Hz). The measurements reveal electrical transport due to ionic impurities as well as three different dipolar relaxations—in addition to the α- and β-relaxation, a slower α'-relaxation is recognized, whose loss peak is disclosed after subtraction of the dc conductivity contribution. The glass transition is found to affect markedly the secondary relaxation, whose strength and shape parameters change across T_g. The major inference from the results concerns the existence of a transition in the dynamics, occurring some tens of degrees above T_g, in the vicinity of the temperature T_S where the peaks of the α- and β-relaxations merge. Evidence in favour of such a transition is given by: (i) the change in the temperature dependence of the α-relaxation time; (ii) independently, the change in the temperature dependence of the dc conductivity; (iii) the breakdown of the Debye–Stokes–Einstein model, replaced at lower temperatures by a fractional regime.

Concerning the α'-process, it shows a Vogel–Fulcher behaviour with the same temperature T_0 as the α-relaxation but, unlike this last, it is not involved in a splitting phenomenon with the β-relaxation. Several hypotheses concerning the nature of the α'-process are explored.

1. Introduction

In a liquid the molecular motions gradually slow down as the temperature is decreased. If crystallization is avoided, the liquid retains a disordered molecular arrangement, and the characteristic relaxation time taken by the system to reach the thermodynamic equilibrium eventually becomes longer than the experimental observation time: in such conditions the molecular motions appear as frozen and the system is said to be a glass. By convention, the entry into the glassy state is settled at the value 10^{13} Poise of the shear viscosity, corresponding to a dielectric relaxation time of 10^2 s. Most systems have dipolar molecular groups which are involved in the motions by which the system relaxes toward the equilibrium state. Consequently, dielectric spectroscopy can be profitably used in the study of relaxation processes occurring in glass-forming systems. In particular, the dielectric response can monitor both structural relaxations, related to motions practically blocked below the glass transition temperature T_g, and secondary relaxations, less sensitive to temperature variations and remaining active in the glassy state.

§ Corresponding author.

0953-8984/99/5010297+18$30.00

For a long time, the attention to the glass transition phenomenon has been focused on a temperature range close to T_g, looking for signs of a phase transition and investigating the microscopic origin of the huge increase of the structural relaxation time. More recently, different theoretical approaches to the glass transition have been adopted [1–5], all involving in some way the existence of a dynamic change well above T_g.

In this renewed perspective, the temperature range of interest in many experimental investigations has shifted to higher temperatures where significant changes in the dynamics should occur [4, 6, 7]; in particular, more attention has been devoted to the splitting region between main and secondary relaxations [8–17]. As in many glass-formers the splitting occurs in the frequency range 10^8–10^9 Hz and the deconvolution of dielectric spectra requires accurate and wideband measurements, considerable efforts have been made to cover wider spectral regions with an improved accuracy [18–21]. Moreover, different variables coupled to the structural dynamics of the systems, i.e. viscosity and dc conductivity [17, 22, 23], and different spectroscopies, such as light scattering [4, 24], neutron spin echo [13], ESR [25] and NMR spectroscopy [7, 26], have also been used to gain additional information.

The comparison among different dynamic observables, such as viscosity, relaxation time and conductivity, is in principle justified by the Debye–Stokes–Einstein relations (DSE) [27, 28]. The validity of these relations in supercooled liquids has been investigated using a number of experimental techniques [4, 6, 17, 22–26, 29–31], giving in some cases evidence of failure [4, 6, 24–26, 29]. Though the origin of DSE violations is still the subject of a heated debate, some connection between the breakdown of the DSE regime and the splitting between dielectric relaxations has been suggested [6].

Within the framework briefly recalled, the present work analyses the dielectric response of a fragile triepoxy glass-former. The temperature behaviour of all the parameters employed in the phenomenological description of the spectra is considered. Epoxy resins are excellent glass-formers, available with various molecular weights [32, 33], and show a strong dielectric response in the supercooled and glassy state, so allowing accurate measurements [17, 19, 23, 34, 35]. On the other hand, dielectric spectroscopy yields independent but simultaneous measurements of dc conductivity and relaxation times, so allowing a reliable check of the DSE model. Besides, conductivity measurements may turn out to be useful in the analysis of the splitting region.

2. Experiment

The chemical compound used in this study was a commercial grade triepoxide (by Aldrich, M.W. = 277.32), N,N-diglycidyl-4-glycidyloxyaniline (DGGOA). The chemical structure (figure 1) comprises three epoxy groups, each having a strong dipole moment (2.1 Debye). No tendency to crystallization was observed for this compound in our experimental conditions. However, even if the sample is stored at low temperature, a very slow polymerization reaction can occur, easily recognizable by a detectable decrease of the conductivity and a slowdown of the relaxation processes. In fact, after using the fresh compound for a first set of measurements and storing the unused fraction for several months, we had to properly filter it in order to restore the characteristics of the fresh compound.

Dielectric measurements were carried out using the HP4194A impedance analyser (10^2 Hz–40 MHz) and the HP8752C network analyser (1 MHz–6 GHz). In the lower frequency range (up to 40 MHz), a stainless steel cylindrical capacitor cell was used (empty cell capacitance, $C_0 \cong 2.4$ pF). In the higher frequency range (from 1 MHz to 6 GHz) the scattering parameters of a transmission coaxial line ended by an open cell (infinite sample configuration) were measured. A cell of relatively high capacitance ($C_0 \cong 0.3$ pF) was chosen

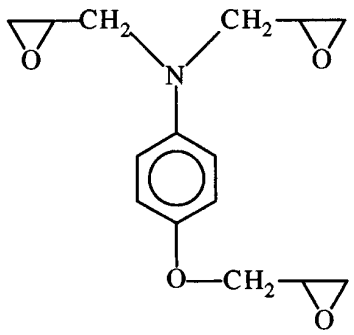

Figure 1. Chemical structure of DGGOA.

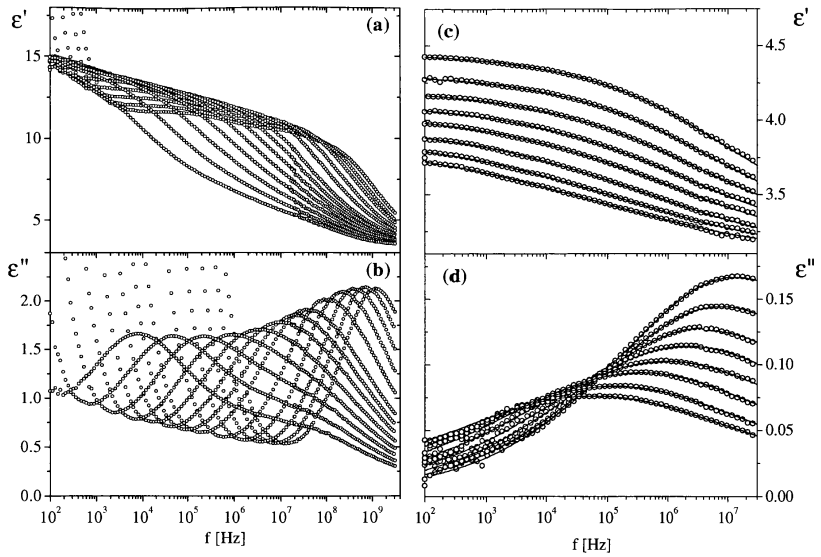

Figure 2. Dielectric spectra: (a) real, ε', and (b) imaginary, ε'', part of the complex dielectric permittivity against frequency for different temperatures (268, 273, 278, 283, 288, 293, 298, 303, 313, 323, 333, 343, 351.5 K) above the glass transition; (c) real, ε'; and (d) imaginary, ε'', part of the complex dielectric permittivity against frequency for different temperatures (165, 173, 183, 193, 203, 213, 223, 233 K) below the glass transition. The solid lines are fitting equations.

in order to obtain a better sensitivity in the MHz region and to assure a sufficient superposition with the data acquired by the impedance analyser. With this choice reliable data were obtained up to 3 GHz. The sample temperature was kept stable within 0.1 K using a conditioned flow of dry nitrogen. Dielectric spectra were acquired in the temperature range from 165 to 351.5 K. For higher temperatures (up to 373 K) only the dc conductivity, σ, was measured. The highest temperature was chosen so that no chemical reaction could occur during the measurements.

3. Results

Figures 2(a) and 2(b) show the frequency dependence of ε' and ε'' for temperatures above T_g in the whole accessible frequency range. Some selected spectra for temperatures below

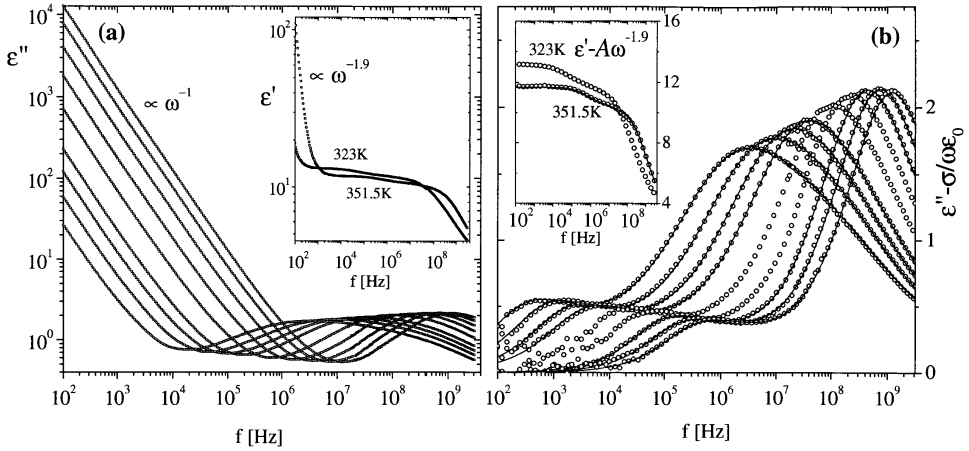

Figure 3. (a) Log–log plot of ε'' against frequency for different temperatures (288, 293, 298, 303, 313, 323, 333, 343, 351.5 K) above the glass transition pointing out the dc conductivity contribution, $\sigma/\omega\varepsilon_0$. The inset shows ε' against frequency on a log–log scale for two selected temperatures; the electrode polarization contribution ($A \times \omega^{-1.9}$) in the low frequency part is apparent. (b) ε'' on a semi-log scale for the same temperatures as in (a), after subtraction of the dc conductivity contribution. The inset shows ε' against frequency on a semi-log scale, after correction for the electrode polarization contribution. The solid lines represent the fitting equation (3).

T_g in the reduced frequency range 10^2–10^7 Hz are drawn in figures 2(c) and 2(d). Below 243 K only one relaxation process, very small and spreading over many frequency decades, is active (secondary or β-relaxation); for higher temperatures both the main (structural or α-) and secondary relaxations are visible in the same experimental window. On heating the system, the α-relaxation shifts toward higher frequencies and eventually merges into the β-process giving rise to an apparently unique relaxation peak. The strong rise $\propto 1/\omega$ ($\omega = 2\pi f$) in the low frequency tail of $\varepsilon''(f)$ for temperatures $\geqslant$273 K (figure 3(a)) reveals a high dc conduction due to the drift of impurity ions.

Above 313 K a strong rise is also seen in the low frequency tail of $\varepsilon'(f)$ (inset of figure 3(a)), probably due to the electrode polarization effect produced by the ions [36–38]. In this case, when ε'' shows a considerable dc conductivity contribution and the electrode polarization effect rapidly decays with frequency, as in our system, the measured apparent permittivity, $\varepsilon'_a - \mathrm{i}\varepsilon''_a$, can be related to the sample permittivity, $\varepsilon' - \mathrm{i}\varepsilon''$, according to the following equations:

$$\varepsilon'_a \cong \varepsilon' + A\omega^{-(N+1)} \tag{1}$$

$$\varepsilon''_a \cong \varepsilon'' = B\omega^{-(N+1)} \tag{2}$$

where A and B are constants depending through σ (see the appendix) on the temperature only, and N ($0 < N < 1$) is the exponent of the power law which represents the electrode polarization effect [36–38]. A demonstration of equations (1) and (2) and the general conditions of their validity are given in the appendix.

Equations (1) and (2) well fit the low frequency values of the permittivity with $N \cong 0.9$ (figure 3(a)); however, the second term in the right-hand side of equation (2) is not appreciable in the ε'' spectra, being smaller than the precision of the data (∼0.1–0.3%). With this we conclude that in our system the electrode polarization effect is well accounted for by a term $\propto\omega^{-1.9}$ in the ε' spectra, while the contribution from dc conduction is well represented by the term $\sigma/\omega\varepsilon_0$ ($\varepsilon_0 = 8.854 \times 10^{-12}$ F m^{-1}, vacuum permittivity) in the ε'' spectra.

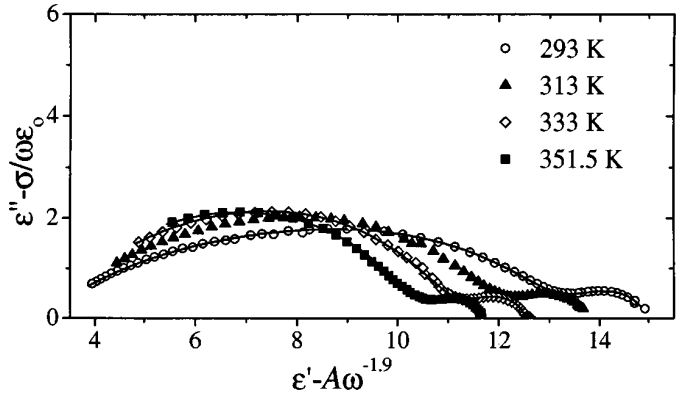

Figure 4. Cole–Cole plots obtained after subtraction of the dc conductivity and electrode polarization contributions. Solid lines from the fitting equation (3).

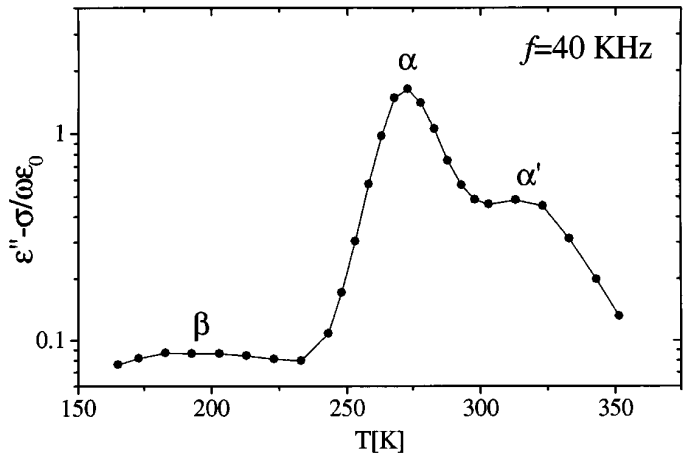

Figure 5. ε'' at the fixed frequency of 40 kHz against temperature. The dc conductivity contribution has been subtracted. The solid line is a guide for the eyes only.

The contributions from both conductivity and electrode effect, evaluated at low frequencies where the dipolar contribution is still negligible, have been subtracted from the ε' spectra at temperatures from 313 to 351.5 K, and from the ε'' spectra at temperatures higher than 288 K; in this way, new spectra like those in figure 3(b) are obtained. It is seen in figure 2(a), and more clearly in the inset of figure 3(a), that a dispersion region in the original ε' spectra occurs at lower frequencies than those of the α-relaxation, but always well separated from the electrode polarization effect. This dispersion obviously remains after subtraction of the electrode polarization (inset of figure 3(b)), and accompanies the loss peak disclosed at the same frequencies in the ε'' spectra (figure 3(b)), thus suggesting the existence of an additional relaxation process. The correlation between the changes in ε' and ε'' is demonstrated by the Cole–Cole plots in figure 4: it is apparent that in addition to the α- and β-relaxation, a slower (α-relaxation contributes to take the electrical polarization back to the equilibrium. Confirmation, beyond all doubt, is given by the temperature dependence of ε'' at fixed frequency (figure 5).

3.1. Data analysis

In the presence of multiple relaxations (typically the α- and β-relaxation) a very controversial issue concerns how to single out the contributions of each process in the splitting region, where there is no clear separation between the peaks. Different approaches are presently debated in the literature [39]. According to the customary additive *ansatz* the overall relaxation function is built as a superposition of individual relaxation functions [11]. Following Williams [40], an alternative *ansatz* in the time domain has been recently proposed [13–15, 41]. In this last, the overall normalized relaxation function $\Phi(t)$ is composed of the normalized relaxation functions for the α- and β-processes $\Phi_\alpha(t)$ and $\Phi_\beta(t)$ in the form $\Phi(t) = A\Phi_\alpha(t) + (1-A)\Phi_\beta(t)\Phi_\alpha(t)$, where A is the fraction of the polarization that relaxes only via the α-process. Even if in principle this approach can be shared, it does not give up the assumption of statistically independent processes, and it still needs certain presuppositions for the shape of the individual relaxation functions. Furthermore, additional assumptions are implied in the extrapolation from low temperatures of the behaviour of $\Phi_\alpha(t)$ and $\Phi_\beta(t)$ in the splitting region [13]. Whatever may be the justification for the choice of one of the two approaches, it is worth noting that in the Williams' *ansatz* the simple superposition is recovered when the α- and β-relaxations are well separated in frequency; in particular, the relaxation times determined from the two different data analyses differ appreciably only when the component processes are less than two decades from each other [11, 14, 15].

For the system here studied, the α'-process is sufficiently separated from the α-process at all temperatures, so that the simple superposition is appropriate to analyse its contribution. Concerning the α- and β-processes, they merge at high temperature and the reliability of the simple superposition may become questionable close to the merging point. However, the additive and the Williams' approaches were compared for an epoxy resin, giving no appreciable differences in the relaxation times when the α- and β-relaxations were separated by more than only one decade [42]. Consequently, the data for the present system were analysed according to the additive approach, giving up fitting the α- and β-processes over 303 K, where their peaks are too close to each other.

The fit procedure has been performed simultaneously on the real and imaginary part of the complex dielectric constant, after subtraction of the electrode polarization and dc conductivity contributions. The three processes α', α and β were represented by the superposition of three Havriliak–Negami (HN) functions [43]:

$$\varepsilon(\omega) - \varepsilon_\infty = (\varepsilon_s - \varepsilon_1)L_1(\omega) + (\varepsilon_1 - \varepsilon_2)L_2(\omega) + (\varepsilon_2 - \varepsilon_\infty)L_3(\omega) \qquad (3)$$

where ε_s and ε_∞ denote the low- and high-frequency limit of the dielectric constant; $\varepsilon_s - \varepsilon_1$, $\varepsilon_1 - \varepsilon_2$ and $\varepsilon_2 - \varepsilon_\infty$ are the dielectric strengths of the α'-, α- and β-process, respectively; $L_j(\omega) = [1 + (\mathrm{i}\omega\tau_j)_j^{1-\alpha}]_j^{-\beta}$ is the normalized HN function, α_j and β_j being the HN shape parameters ($j = 1, 2, 3$ refer to α'-, α- and β-process, respectively).

The presence of three relaxation processes requires a large number of adjustable parameters and great caution in the fit procedure. However, as the α'-process is sufficiently separated from the others, it was easily subtracted from the spectra, so that only the α- and β-processes were fitted together. Subsequent tests confirmed that the fitting parameters obtained from such procedure and from the three-relaxation function (equation (3)) perfectly agree. On the other hand, reliable fits with three relaxations are reported in the literature [16, 44, 45]. We note that the number of fitting parameters has sometimes been reduced by the assumption of symmetry for the secondary process ($\beta_3 = 1$) [13, 14, 46], or by extrapolation of the shape parameters from their values below T_g [13, 14]. Since previous studies on different epoxy compounds have shown a significant and temperature-dependent asymmetry of the secondary relaxation [19, 23], here we have preferred to not assume any specific symmetry condition for this process,

either above or below the glass transition. The solid lines in figure 3(b) and 4 are the best fits obtained using equation (3).

By following the analysis criteria so far explained the conductivity σ, the strength, the characteristic time τ and the shape parameters α and β for each process have been determined at various temperatures. Details are reported in the following subsections.

A sensitive temperature-derivative method recently proposed by Stickel and co-workers [47] has been adopted in the analysis of the temperature behaviour of conductivity and structural relaxation time. The method rests on the observation that the Vogel–Fulcher- (VF-) type behaviour of a generic observable $x(T)$, i.e. $x = x_0 \exp(-B/(T - T_0))$, is linearized by the new variable $\Phi_x \equiv (\mathrm{d}\log_{10} x/\mathrm{d}T)^{-1/2}$ as a function of T. This representation amplifies changes of behaviour only weakly seen in the Arrhenius plot and allows the comparison on the same scale of different observables in spite of different pre-exponential factors, provided that the data are accurate enough to support the numerical procedure.

3.2. Conductivity

Ionic impurities, such as Na^+ and Cl^- ions and other chloride derivatives, are generally present in commercial samples of epoxy resins as residues of their synthesis, in typical concentrations of tens of ppm. To these impurities is generally attributed the observed dc conductivity in this class of materials. The conductivity parameter σ of DGGOA was determined in the temperature range 268–373 K. In many cases, an empirical VF-like function, $\sigma = \sigma_0 \exp(-B/(T - T_0))$, has been used to reproduce the temperature behaviour of conductivity [32, 33]. More recently, however, for a great number of low molecular weight glass-forming liquids a similar function has been found to not represent properly the experimental behaviour over the whole temperature range above T_g [17, 22, 23].

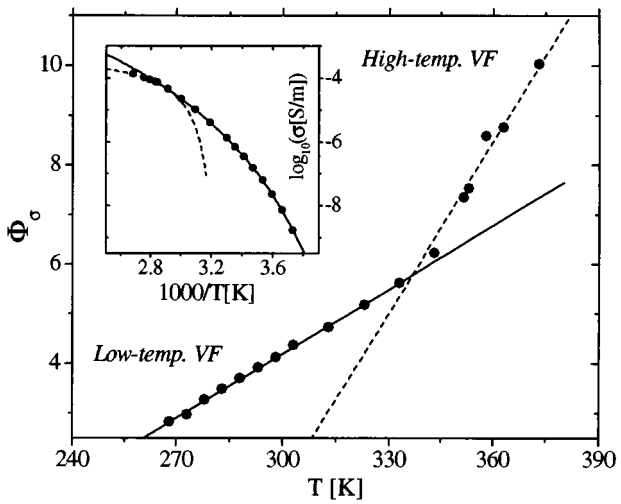

Figure 6. The quantity $\Phi_\sigma = [\mathrm{d}\log_{10}(\sigma)/\mathrm{d}T]^{-1/2}$ against T. The solid and dashed straight lines represent a description of the data in terms of two VF laws (the fitting parameters are listed in table 1). In the inset: dc conductivity, σ, against the reciprocal temperature.

In order to obtain a deeper insight into the conductivity behaviour in a model-independent way, the plot of the quantity $\Phi_\sigma(\mathrm{d}\log_{10}\sigma/\mathrm{d}T)^{-1/2}$ represents a very powerful tool (figure 6). Near $T_\sigma \sim 336$ K a marked change of slope is seen, which suggests a description of the data

Table 1. Fitting parameters of the VF law, $x = x_0 \exp[-B/(T - T_0)]$, for the indicated quantities.

x-variable	Temperature range	x_0 (same unit as for x)	B (K)	T_0 (K)
σ (S m^{-1})	268 K $< T \leqslant$ 333 K	0.24 ± 0.08	1200 ± 60	204 ± 2
σ (S m^{-1})	333 K $< T <$ 373 K	$(7.8 \pm 2.3) \times 10^{-4}$	140 ± 30	292 ± 6
$\tau_{\alpha'}^{-1}$ (s^{-1})	263 K $< T \leqslant$ 333 K	$(9 \pm 4) \times 10^{9}$	1300 ± 70	206 ± 2
τ_{α}^{-1} (s^{-1})	268 K $< T \leqslant$ 333 K	$(1.6 \pm 0.5) \times 10^{14}$	1450 ± 50	205 ± 1
τ_{α}^{-1} (s^{-1})	333 K $< T <$ 373 K	$(9 \pm 4) \times 10^{10}$	210 ± 70	280 ± 10

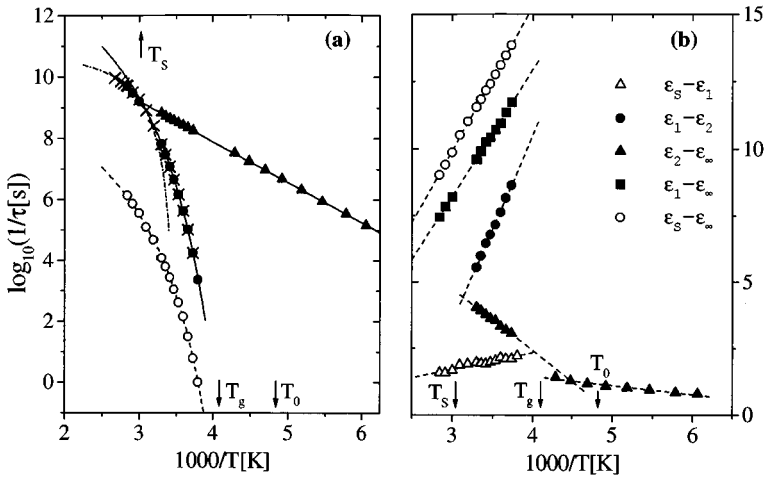

Figure 7. (a) Dielectric relaxation time τ of the α'- (open circles), α- (full circles) and β- (triangles) relaxation plotted against the reciprocal temperature. Crosses indicate the values of the α-relaxation time calculated from dc conductivity data, τ_σ. The solid and dash–dotted lines represent the best description of the α-relaxation time in terms of two VF laws (see figure 10 below—the fitting parameters are listed in table 1); the straight line is the best Arrhenius fit to the β-relaxation time; the dashed line is the VF fitting equation of the α'-relaxation time. (b) Dielectric relaxation strengths plotted against the reciprocal temperature: overall strength (open circles) and strengths of the α'- (open triangles), α- (full circles) and β- (full triangles) relaxation.

The splitting temperature, $T_S \sim 330$ K, the glass transition temperature, $T_g = 244$ K, and the VF temperature, $T_0 = 205$ K, are indicated.

in terms of two different VF regimes as indicated by the solid and dashed lines. The VF fitting parameters are reported in table 1. Similar results were previously found in different epoxy compounds [17, 23].

3.3. α'-process

The α'-relaxation is visible in the ε' and ε'' spectra from 263 up to 351.5 K. By decreasing the temperature this process rapidly shifts towards lower frequencies, showing a VF temperature dependence, $\tau = \tau_0 \exp(B/(T - T_0))$, of its characteristic time, $\tau_{\alpha'}$ (dotted line in figure 7(a)). The VF fitting parameters are listed in table 1; in particular, the temperature $T_0 = 206 \pm 2$ K coincides within the errors with the temperature $T_0 = 204 \pm 2$ K of the VF fit of the conductivity in the low temperature regime.

The shape of the relaxation is almost temperature independent (figure 8(a)), with the loss peak slightly broader ($\alpha_1 \approx 0.2$) compared to a Debye relaxation, but very asymmetric ($\beta_1 \approx 0.4$). A relaxation strength $\varepsilon_s - \varepsilon_1$ slightly decreasing with temperature roughly according to a $1/T$ dependence is found (figure 7(b)).

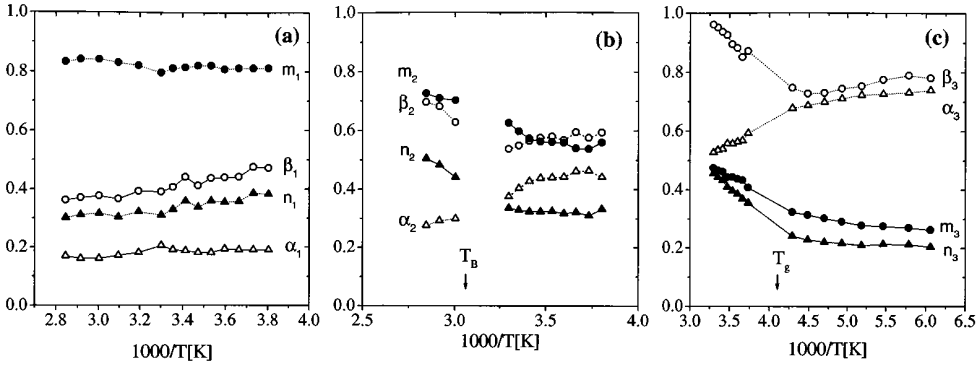

Figure 8. Temperature dependence of the HN shape parameters, α and β, of the (a) α'-, (b) α- and (c) β-relaxation. The lines are only guides for the eye. (For the meaning of T_B see the discussion.) For a comparison, the parameters $m = 1 - \alpha$ and $n = (1 - \alpha)\beta$, which are the exponents of the power laws describing ε'' in the low and high frequency limit, respectively, are also shown.

3.4. α- and β-processes

Whereas the α'- and α-relaxation remain separated in frequency by more than three decades, the α- and β-relaxation approach each other when the temperature increases, and eventually they merge. The characteristic time of the β-process (triangles in figure 7(a)) follows an Arrhenius temperature behaviour with activation energy $E_a = 6.0 \pm 0.1$ kcal mol^{-1}, while the relaxation time of the α-process (solid circles in figure 7(a)) shows a stronger temperature dependence which, for temperatures not too high, can be represented by a VF law with $\tau_0 = (6.3 \pm 1.9) \times 10^{-15}$ s, $B = (1450 \pm 50)$ K and $T_0 = 205 \pm 1$ K (see table 1).

The extrapolation of the Arrhenius fitting curve intersects the VF fitting curve at $T_S \sim 330$ K (splitting temperature), where the relaxation time is about 1 μs (figure 7(a)). Consequently, at temperatures higher than T_S only one HN term was considered. We note that the analysis of the spectra above T_S in terms of a unique HN function does not appreciably change the values of the structural relaxation time and does not affect the conclusions on the relaxation dynamics drawn in the following. In recent years, the need of caution in the interpretation of the merging of the α- and β-process has been emphasized by models [48, 49] and by means of alternative data analyses (see section 3.1) that make it difficult to define a splitting temperature in an unambiguous way. We are fully aware that the temperature T_S, relying on extrapolation, may represent a reference temperature only, in the sense that a real merging of the α- and β-process does not necessarily take place at T_S. Anyway, within the overall picture some features will point to T_S as some physical indicator.

Here we note that both the α'- and α-processes slow down by cooling the system and both of them can be classified as structural processes, being related to molecular motions which freeze at the glass transition. Looking at table 1, it is worth stressing that the limit VF temperature, T_0, is the same for all the structural dynamic processes of our system (i.e. electrical transport, α'- and α-relaxation). When the dielectrometric definition of glass transition temperature, $\tau(T_g) = 10^2$ s, is applied, it yields sensibly different values from the fitting equation of τ_α or $\tau_{\alpha'}$, resulting in $T_g(\alpha) = 244 \pm 2$ K and $T_g(\alpha') = 253 \pm 3$ K. We consider $T_g(\alpha)$ as a more appropriate value for the glass transition temperature of DGGOA, because the α-relaxation is the faster process associated with those molecular motions frozen by cooling the system.

The shape of the α-relaxation between T_g and T_S is found to be quite stable (figure 8(b)), while its strength, $\varepsilon_1 - \varepsilon_2$, strongly decreases linearly with $1/T$ on heating the system (figure 7(b)). Concerning the β-process, its shape, almost unchanged below T_g, changes

across the glass transition, becoming more symmetric and narrow as the temperature increases (figure 8(c)). The strength, $\varepsilon_2 - \varepsilon_\infty$, is found to increase with temperature, very slowly below T_g and more steeply above T_g (figure 7(b)). Such increase could be due to an increase of the number of relaxing dipoles [50] or, assuming that all molecules participate in the β-process [41], to an increase of the angle of reorientational motion of the dipoles. Even though the nature of the secondary process is far from being clear, the observation that the relaxation strength of this process is enhanced by a release of degrees of freedom of the whole molecule above T_g points toward a significant intermolecular contribution to the motions underlying the secondary process.

4. Discussion

The investigation of the molecular dynamics in glass-forming fluids can be carried out by dielectric spectroscopy gaining information from the simultaneous measurement of both conductivity, which probes a translational diffusion mechanism of charge carriers, and relaxation times, which are related to a rotational mechanism of dipoles. Both observables reflect the mobility of molecular species but are related to different motions whose coupling is not obvious in principle. Thus, the relationships given in the literature between the dielectric relaxation and the charge transport processes cannot be generally taken as predictive and they should be experimentally verified.

In this respect, the classical Stokes–Einstein and Debye–Stokes relations relate to each other's various transport coefficients, i.e. $D \propto T/\eta$, $D_i \propto T\sigma$ and $\tau \propto \eta/T$ (where D is the self-diffusion coefficient, η the shear viscosity, σ the dc conductivity, D_i the ionic diffusion coefficient and τ the orientational diffusion time), within a simple and very general model derived for a macroscopic particle diffusing in a continuous medium (hydrodynamic regime) [27, 28]. Considering that in the supercooled state τ and η vary over many orders of magnitude in a relatively narrow temperature range, the approximated relation $\tau \propto \eta$ can be used up to temperatures where the $1/T$ dependence can be neglected [20], and the following Debye–Stokes–Einstein (DSE) relation is obtained between σ and τ:

$$\sigma\tau \cong \text{constant}. \tag{4}$$

Equation (4) has been well verified in ordinary liquids as well as in many simple glass-forming fluids in the supercooled regime [17, 22, 23], irrespective of the fact that it should be strictly valid for diffusing particles larger than the surrounding molecules. During recent years, the existence of appreciable deviations from the DSE behaviour in deeply supercooled liquids has been documented by a number of experimental works [4, 6, 24–26, 29, 33, 35, 51–54], and it has been variously depicted as a signal of the dynamic phase transition predicted by the mode-coupling theory (MCT) [1, 6, 7, 55] or ascribed to the onset of cooperative motions [4]; sometimes [31, 56–60], the formation of structured domains in the supercooled fluid has been invoked. Whatever is the picture, the departure from the DSE regime can be taken as a strong indicator for a change of the diffusion mechanism.

The check of equation (4) is shown for the α'- and α-process in figure 9. In the log–log representation the DSE behaviour corresponds to a straight line with slope -1. The linear fit yields a slope $s = 0.87 \pm 0.01$ for the data of the α'-process (figure 9(a)), while the data of the α-process do not exhibit a unique value of s over the whole data set (figure 9(b)). Only the data at the highest temperatures fulfil the prediction of the DSE model (the linear regression yields $s = 0.99 \pm 0.03$), whereas the data below 303 K are described with a high degree of accuracy by a straight line with $s = 0.814 \pm 0.006$. The two fitting straight lines in figure 9(b) intersect at

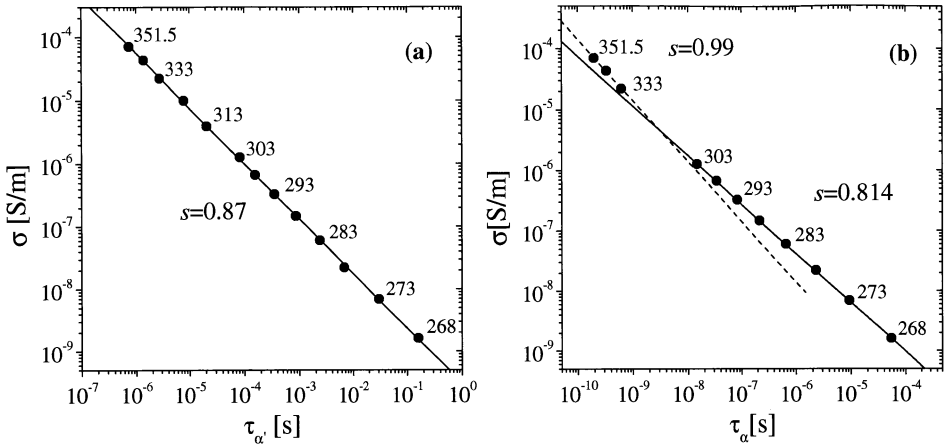

Figure 9. Dc conductivity (a) against the relaxation time of the α'-process, $\tau_{\alpha'}$, and (b) against the relaxation time of the α-process, τ_α, on a log–log plot. The solid lines represent the fitting equation $\sigma\tau^s = \text{constant}$. The dashed line is the DSE law (equation (4)).

about 320 K. When equation (4) fails, our results support the validity of the following equation:

$$\sigma\tau^s = \text{constant} \tag{5}$$

with s less than 1 (fractional Debye–Stokes–Einstein law, FDSE), successfully employed to describe similar deviations from the DSE model in supercooled liquids [24, 25, 29, 33, 35, 52, 53]. It is tempting to read the fractional exponent s within the free volume theory [29, 61–63] as the ratio between the critical free volume for the ionic transport, v_σ^*, and the critical free volume for the dipolar orientation, v_τ^* [33, 51]. Values of $s < 1$ then correspond to a dynamic regime where a greater v_τ^* compared to v_σ^* is required. However, in spite of various attempts made so far [4, 31, 52, 56, 57, 64], a rigorous theoretical derivation of power law relations with a fractional exponent has not yet been achieved, and such relations should be better taken as phenomenological descriptions.

Since a failure of the DSE model is expected to occur at low temperatures [22], the validity of equation (4) toward higher temperatures, and particularly above 351.5 K (upper temperature limit for the measured relaxation times), can be assumed and employed to calculate additional relaxation times up to 373 K. In figure 7(a) crosses indicate the values τ_σ calculated by scaling the values of σ according to equations (4) and (5), using the exponent s and the constant on the right-hand side of these equations as obtained from the best fits in figure 9(b). This widens the range of the structural relaxation time to values otherwise not easily accessible by dielectric relaxation measurements, and also covers the splitting region. The representation of the structural relaxation times through the variable $\Phi_{1/\tau} = [\mathrm{d}\log_{10}(1/\tau)/\mathrm{d}T]^{-1/2}$, that linearizes the VF equation as a function of T, shows a marked change of slope around $T_B \sim 332$ K (figure 10), very close to the temperature ($T_\sigma \sim 336$ K) where a similar behaviour is observed in Φ_σ. Again, the data can be suitably described by assuming two different VF laws (see parameters in table 1), similarly as found by Stickel *et al* [22]. Incidentally, we observe that the behaviour of Φ_σ and $\Phi_{1/\tau}$ reflects the coupling between σ and τ shown in figure 9(b) [65]. We point out that the sharp bend in the trend of Φ is a model-independent result, i.e. identified independently of the use of VF equations to describe the low and high temperature data. Alternative descriptions are possible indeed [21]. Moreover, it has to be stressed that the information provided by conductivity and relaxation times are independent of

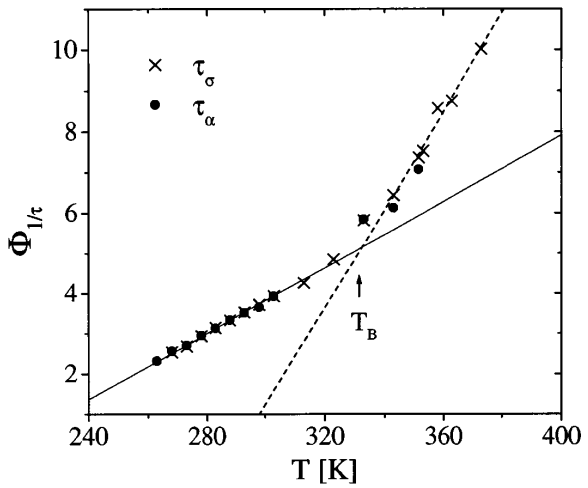

Figure 10. The quantity $\Phi_{1/\tau} = [\mathrm{d}\log_{10}(1/\tau)/\mathrm{d}T]^{-1/2}$ against T for the α-process. The relaxation time data are from direct measurements, τ_α (full points), and calculated from conductivity, τ_σ (crosses).

each other; in fact, the values of σ are obtained from the low frequency region of the spectra, well separated from the relaxation contribution whose fit determines the values of τ. It is noteworthy that the temperature $T_B \sim 332$ K where the change of slope is seen in figure 10 coincides, within the experimental errors, with the splitting temperature T_S, in agreement with previous observations in other glass-forming liquids [16, 17, 23]. Besides, the DSE breakdown occurs across the temperature region where also T_B and T_σ are located.

The most interesting result is that all the various mentioned phenomena take place within a very small temperature range. These our findings allow a unified picture indicating a significant change of the dynamics in the supercooled state, and also they support the suggestion of some connection with the time decoupling between the main and secondary dielectric relaxations [6].

The interpretation of experimental results concerning the existence of a change above T_g in the dynamics of supercooled liquids is a very controversial matter. As a fact, MCT is the only fully microscopic theory of the glass transition presently available, and certain aspects of our results qualitatively agree with MCT predictions. The idealized version of MCT predicts a structural arrest at a critical temperature T_C where an ergodic–nonergodic transition should occur. The absence of critical behaviour at T_C observed in real systems is expected within the extended MCT [2], where the structural arrest is avoided due to phonon-assisted hopping processes that restore ergodicity below T_C. In this view, the bending of Φ reported in figure 6 and figure 10 then marks the crossover from liquid-like diffusional motion to solid-like jump processes addressed by the extended theory. Also the decoupling phenomenon between translational and rotational diffusion described in figure 9 can be qualitatively understood in terms of the same change of motional mechanism: for $T > T_C$ MCT predicts the validity of equation (4), since a relaxation time which scales with viscosity is expected for each quantity that couples with density fluctuations; for $T < T_C$ different hopping rates may characterize different molecular motions (conduction and dipolar orientation). The values of the shape parameters of the α-relaxation (figure 8(b)) are likely to confirm a difference in the relaxation process on crossing the temperature region where the DSE breakdown, the change in the temperature behaviour of τ and the splitting take place: in fact, the time–temperature

superposition appears not to be recommended for this process on crossing this region. Overall, our analysis indicates that significant dynamic peculiarities occur in a small temperature range around $\sim 1.35 T_g$, not far from the values estimated for T_C in fragile liquids by different experiments: $T_C \sim 1.15$–$1.3 T_g$ [6, 7, 52, 54, 66, 67].

If a more quantitative agreement with experimental data is looked for, one faces the problem that MCT has yet to overcome several basic questions which make its applicability to dielectric phenomena still a matter of controversy. In fact, the dielectric results should be compared quantitatively to a theory including orientational degrees of freedom of dipolar molecules, but in its present version MCT does not allow for the slow β-process and the related α–β splitting phenomenon. Moreover, the behaviour in the deeply supercooled state should be compared with the extended MCT, but the dynamical equations considered in that version of the theory have not been solved so far in the low temperature regime.

On the other hand, the overall phenomenology could be qualitatively rationalized using the concept of cooperativity with a characteristic length scale increasing for decreasing temperatures [5]. The splitting is natural in this picture, as marking the onset of cooperative molecular motions: an increasing cooperativity controls the structural α-process leading to increasing apparent activation energies, while local modes are responsible for the simple activated β-process. The change in the temperature behaviour of τ (figure 10) and the shape parameters (figure 8) then reflects the *ansatz* that the α-process below the splitting is a rather independent phenomenon, having its own properties with respect to the unique process above T_S [10, 68]. In particular, within the thermodynamic fluctuation theory [3] cooperativity gives rise to VF behaviour of the α-process, therefore a change in the temperature dependence of τ is expected above T_S where cooperativity breaks down. The DSE breakdown (figure 9) can be interpreted as the crossover from diffusion in a liquid-like non-cooperative regime to diffusion in a dynamically heterogeneous system.

The temperature dependence of the dielectric strengths as well has been considered important for a physical interpretation of the results within the cooperativity picture [9–12]. As a general remark, with decreasing temperature an increasing intensity for the cooperative α-process and a decreasing intensity for the local β-process are expected in the cooperativity view. A similar scenario is experimentally observed in figure 7(b). On the other hand, experimental evidence of vanishing intensity of the α-component in the splitting region for several polymers has made attractive the idea that the cooperativity onset is accompanied by a dielectric onset ($\Delta\varepsilon_\alpha \equiv \varepsilon_1 - \varepsilon_2 \to 0$ for $T \to T_S$) [9–12]. Figure 7(b) clearly shows that the α-intensity is not vanishing at T_S in the present system. This and similar results observed in other substances [9, 23, 69] cast doubts on the necessity of associating the onset of cooperativity with $\Delta\varepsilon_\alpha = 0$ and support a more varied scenario like that discussed in [9].

Overall, at least a qualitative agreement of some basic aspects of the present results with both MCT and cooperativity model can be stated, in particular concerning a change of motional mechanism at some critical point well above T_g; however, it is not possible to argue in favour of one theory or another on the basis of only the data here reported due to a lack of quantitative predictions for the dielectric response of deeply supercooled complex systems. At present different explanations may be possible. Admittedly, whereas the cooperativity picture assumes rather than proves an onset of cooperative motions, in MCT the concept of critical temperature comes from the theory itself.

Some additional comments have to be made about the nature of the α'-relaxation, which we have classified as a structural process, being related to molecular motions that are frozen at the glass transition. Some features of this process are worth recalling: (a) its characteristic time diverges at the same temperature T_0 as for the conductivity σ and the α-relaxation time; (b) this process is much slower than the α-relaxation, $\tau_{\alpha'}$ being at least three order

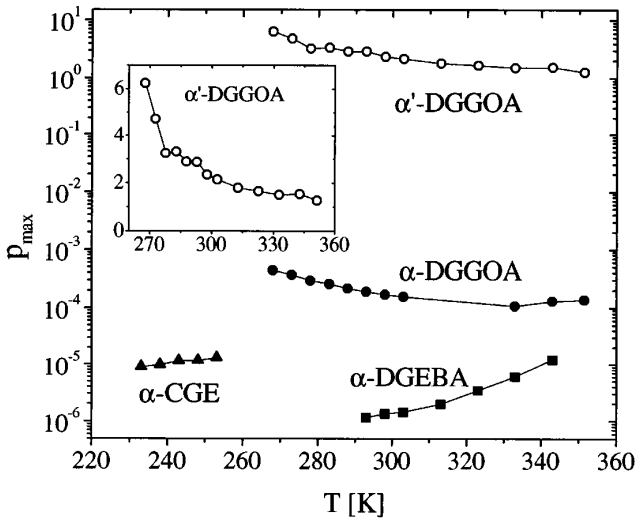

Figure 11. Temperature dependence of the correlation factor $p_{max} = \sigma/\varepsilon_0 \Delta\varepsilon\omega_{max}$. Data are from the α-relaxation in CGE (triangles) [23], DGEBA (squares) [17] and DGGOA (full circles), and from the α'-relaxation in DGGOA (open circles). The inset shows p_{max} for the α'-relaxation on a linear scale.

of magnitude longer than τ_α in the whole temperature range investigated; (c) it does not appear directly linked to the β-relaxation by a splitting phenomenon (figure 7(a)); (d) the value of the exponent s in equation (5) for this process is comparable to that obtained for the α-relaxation (figure 9); finally, (e) its shape is almost temperature invariant and far from that of a Debye process.

Multiple dielectric relaxations related to the structural dynamics were previously observed in both polymeric and low molar mass systems [37, 70, 71]. Since DGGOA is not a polymeric system, the often-invoked Rouse theory for normal modes [70, 71] cannot be considered here. For flexible complex organic molecules, slow molecular motions involving dipolar groups with considerable steric hindrance were assumed as responsible of multiple structural relaxations (see [37]—page 357, and references therein). In our case, the α'-relaxation is so much slower than the α-relaxation as to discourage a similar attribution, though this is not unreasonable.

There are two further hypotheses, previously used to account for similar processes, which consider the effects of the dynamics of electric charge carriers: they are (i) the presence of Maxwell–Wagner polarization [72] and (ii) the contribution of charge carrier relaxation [73–75]. In several cases, relaxations observed at frequencies lower than those of the α-relaxation have been attributed to Maxwell–Wagner effects [45, 72, 76] due to interfacial polarization at the boundaries between regions of the system with very different dielectric properties. However, under the experimental conditions adopted, it is difficult to admit the presence of an intrinsic macroscopic heterogeneity in our samples, and thus a Maxwell–Wagner origin for the α'-process seems quite unlikely. In favour of the second hypothesis there is the fact that, in contrast to the α-relaxation, the α'-loss peak is masked at any temperature by the dc conductivity contribution, and also its position coincides with that of the loss peak predicted for the conductivity relaxation in disordered systems [73]. Moreover, the α'-relaxation matches all the features considered as typical for dispersive processes associated to the charge transport in inhomogeneous conductors [73–75, 77]: (i) the apparent activation energy is nearly the same

as for the dc conduction; (ii) the shape of the relaxation is almost constant with temperature (figure 8(a)); (iii) the relaxation time distribution is broad; (iv) the dielectric strength is not strongly affected by temperature (figure 7(b)); (v) the correlation factor $p_{max} = \sigma/\varepsilon_0 \Delta\varepsilon\omega_{max}$ between dielectric relaxation and dc conduction (ω_{max} is the angular frequency of the loss peak) is of the order of unity. Concerning the point (v), it must be noticed that the α'-relaxation is the only structural process, among those observed in a set of epoxy compounds [19, 23], for which p_{max} is of the order of unity, despite of its slight temperature dependence, while for the other processes p_{max} is smaller by three to six orders of magnitude (figure 11). Moreover, DGGOA has a chemical structure with strong dipolar groups branched around the benzene ring (figure 1), which can favour the formation of weak bonds and the trapping or the localization of ionic carriers; this might be the cause of a dispersive behaviour of the charge transport. Anyway, all these considerations should be better regarded as a starting point for further investigations in order to settle the question about the nature of the α'-relaxation.

5. Conclusions

The system here investigated shows two structural (α- and α'-) relaxations, a secondary one and also contains ionic species which drift under the action of an electric field. The temperature behaviour of conductivity as well as of other relaxation parameters, i.e. relaxation times, strengths and shape parameters, has been carefully analysed. The analysis of the splitting region, very controversial on the basis of only relaxation data, significantly gains from conductivity measurements. The main inference concerns the existence of two transitions characterizing the dynamics of the system in the supercooled state: the glass transition at T_g, corresponding to the entry into the glassy phase, where the system can no longer restore its equilibrium state within the experimental time window, and a further transition, occurring in a narrow temperature range well above T_g ($\sim 1.35 T_g$), which is common to conductivity and to polarization dynamics. The glass transition markedly affects the secondary relaxation, whose strength and shape parameters change across T_g. The transition at higher temperature is signalled, from the dielectric point of view, by a marked change in the temperature behaviour of both conductivity (crossing temperature $T\sigma \sim 336$ K) and α-relaxation time (crossing temperature $T_B \sim 332$ K), by the breakdown of the DSE relation (transition temperature $\sim$320 K), and by the splitting between the structural and secondary relaxation processes (splitting temperature $T_S \sim 330$ K). The overall phenomenology can be qualitatively considered in relation with the change of motional mechanism discussed by MCT, or with the onset of cooperative motions involved by several pictures of the glass transition. Anyway, at present no theory is able to fully explain the experimental findings, and more work is needed to bridge the gap still existing between theoretical predictions and real complex systems. In particular, all theoretical approaches are lacking in quantitative predictions concerning the breakdown phenomenon, and none of them addresses the question of the correlation between the structural and the secondary process.

In advance of many questions that still remain open, more accurate experimental studies and a larger database are required to make progress. In this connection, we stress that our results give a full phenomenological picture by means of a unique technique, thus bypassing the problems related to the lack of direct connection among the physical quantities sensed by different experimental methods. As a fact, a similar coherent picture can be only drawn for *o*-terphenyl, resting on data from different techniques [4, 6, 52, 55, 66].

Finally, we think that the present work may add new experimental material to a very wide and debated field, and it may contribute to increase the interest in thoroughly exploring the temperature region above T_g where many features in the dynamics of glass-forming systems

announce the approaching of the glassy state. Further investigations on other compounds with an increasing number of epoxy groups are presently in progress in our laboratory.

Acknowledgments

The authors are grateful to Dr R Casalini and Dr D Fioretto for many helpful discussions.

This work was partially supported by funds of Ministry of University and Scientific and Technological Research (MURST).

Appendix. Correction for the electrode polarization effect

The presence of high ionic conductance is often liable for electrode polarization effects at the lowest frequencies. In this case, the equivalent circuit representing the electric response of the system is formed by a complex impedance, Z_{el}, in series with the sample impedance $Z = 1/[\mathrm{i}\omega C_0(\varepsilon' - \mathrm{i}\varepsilon'')]$, so that the apparent permittivity, $\varepsilon'_a - \mathrm{i}\varepsilon''_a$, can be described by the following equation [37]:

$$\varepsilon'_a - \mathrm{i}\varepsilon''_a = \frac{\varepsilon' - \mathrm{i}\varepsilon''}{1 + \mathrm{i}\omega C_0(\varepsilon' - \mathrm{i}\varepsilon'')Z_{el}} \tag{A1}$$

where C_0 is the empty capacitance of the cell containing the sample. A strong interest in dielectric studies is to eliminate the disturbances due to the electrode polarization effects from the measured permittivity $\varepsilon'_a - \mathrm{i}\varepsilon''_a$.

Concerning this, every time that the following conditions are fulfilled: $\varepsilon'' \gg \varepsilon'$ and $|Z_{el}|\omega C_0\varepsilon'' \ll 1$ (these two conditions are physically equivalent to requiring that the electrode impedance $|Z_{el}|$ is negligible compared to the sample impedance), the following approximation is valid:

$$\varepsilon'_a - \mathrm{i}\varepsilon''_a \cong (\varepsilon' - \mathrm{i}\varepsilon'')[1 - Z_{el}\omega C_0\varepsilon'']. \tag{A2}$$

Usually, in systems where ε'' is dominated by the conductivity and the electrode impedance Z_{el} rapidly decays at higher frequencies, the above cited conditions for the validity of equation (A2) are fulfilled in a wide frequency range, and therefore equation (A2) provides a good basis for a simple correction for the electrode polarization effect. The electrode impedance can be represented as a partly capacitive and partly resistive element; following the usual assignment $Z_{el} = A_0(\mathrm{i}\omega)^{-N}$ [36–38], where A_0 is a constant characteristic of the electrode/material interface and $0 < N < 1$, equation (A2) yields:

$$\varepsilon'_a \cong \varepsilon' + \left(A_0 \sin N\frac{\pi}{2}\right)\omega^{-(N+1)}(\omega^2 C_0\varepsilon''^2) \tag{A3}$$

$$\varepsilon''_a \cong \varepsilon'' - \left(A_0 \cos N\frac{\pi}{2}\right)\omega^{-(N+1)}(\omega^2 C_0\varepsilon''^2). \tag{A4}$$

In equations (A3) and (A4) ε'' is the superposition of the dipolar relaxation and conductivity contributions. When the dipolar term is negligible compared to the conductivity term, so that $\varepsilon'' \cong \sigma/\omega\varepsilon_0$ (with $\varepsilon_0 = 8.854 \times 10^{-12}$ F m^{-1} vacuum permittivity), the electrode polarization effect can be simply described by means of the equations:

$$\varepsilon'_a = \varepsilon' + \left(\frac{A_0 C_0\sigma^2}{\varepsilon_0^2} \sin N\frac{\pi}{2}\right)\omega^{-(N+1)} \tag{A5}$$

$$\varepsilon''_a = \varepsilon'' - \left(\frac{A_0 C_0\sigma^2}{\varepsilon_0^2} \cos N\frac{\pi}{2}\right)\omega^{-(N+1)} \tag{A6}$$

which are equivalent to equations (1) and (2) introduced in section 3 of this paper, with $A = (A_0C_0\sigma^2/\varepsilon_0^2)\sin(N\pi/2)$ and $B = (A_0C_0\sigma^2/\varepsilon_0^2)\cos(N\pi/2)$.

References

[1] Götze W and Sjögren L 1992 *Rep. Prog. Phys.* **55** 242
[2] Götze W and Sjögren L 1988 *J. Phys. C: Solid State Phys.* **21** 3407
[3] Donth E 1992 *Relaxation and Thermodynamics in Polymers: Glass Transition* (Berlin: Akademie)
[4] Fischer E W, Donth E and Steffen W 1992 *Phys. Rev. Lett.* **68** 2344
[5] Donth E 1996 *J. Polym. Sci.*B **34** 2881
[6] Rössler E 1990 *Phys. Rev. Lett.* **65** 1595
[7] Rössler E, Tauchert J and Eiermann P 1994 *J. Phys. C: Solid State Phys.* **98** 8173
[8] Garwe F, Schönhals A, Beiner M, Schröter K and Donth E 1994 *J. Phys.: Condens. Matter* **6** 6941
[9] Garwe F, Schönhals A, Lockwenz H, Beiner M, Schröter K and Donth E 1996 *Macromolecules* **29** 247
[10] Beiner M, Korus J and Donth E 1997 *Macromolecules* **30** 8420
[11] Schröter K, Unger R, Reissig S, Garwe F, Kahle S, Beiner M and Donth E 1998 *Macromolecules* **31** 8966
[12] Beiner M, Kahle S, Hempel E, Schröter K and Donth E 1998 *Macromolecules* **31** 8973
[13] Arbe A, Richter D, Colmenero J and Farago B 1996 *Phys. Rev.* E **54** 3853
[14] Alvarez F, Hoffman A, Alegría A and Colmenero J 1996 *J. Chem. Phys.* **105** 432
[15] Bergman R, Alvarez F, Alegría A and Colmenero J 1998 *J. Chem. Phys.* **109** 7546
[16] Hansen C, Stickel F, Berger T, Richert R and Fischer E W 1997 *J. Chem. Phys.* **107** 1086
[17] Capaccioli S, Corezzi S, Gallone G, Rolla P A, Comez L and Fioretto D 1998 *J. Non-Cryst. Solids* **235–237** 576
[18] Hofmann A, Kremer F, Fischer E W and Schönhals A 1994 *Disorder Effects on Relaxational Processes* ed R Richert and A Blumen (Berlin: Springer) pp 309–21
[19] Casalini R, Fioretto D, Livi A, Lucchesi M and Rolla P A 1997 *Phys. Rev.* B **56** 3016
[20] Hansen C, Stickel F, Richert R and Fischer E W 1998 *J. Chem. Phys.* **108** 6408
[21] Schneider U, Lunkenheimer P, Brand R and Loidl A 1999 *Phys. Rev.* E **59** 6924
[22] Stickel F, Fischer E W and Richert R 1996 *J. Chem. Phys.* **104** 2043
[23] Corezzi S, Capaccioli S, Gallone G, Livi A and Rolla P A 1997 *J. Phys.: Condens. Matter* **9** 6199
[24] Comez L, Fioretto D, Verdini L, Rolla P A, Gapinski J, Patkowski A, Steffen W and Fischer E W 1999 *Phys. Rev.* E **60** 3086
[25] Andreozzi L, Di Schino A, Giordano M and Leporini D 1996 *J. Phys.: Condens. Matter* **8** 9605
[26] Chang I and Sillescu H 1997 *J. Phys. Chem.* B **101** 8794
[27] Einstein A 1905 *Ann. Phys, NY* **17** 549
[28] Debye P 1929 *Polar Molecules* (London: Dover)
[29] Ehlich D and Sillescu H 1990 *Macromolecules* **23** 1600
[30] Menon N, Nagel S R and Venerus D C 1994 *Phys. Rev. Lett.* **73** 963
[31] Cicerone M T, Blackburn F R and Ediger M D 1995 *J. Chem. Phys.* **102** 471
[32] Sheppard N F Jr and Senturia S D 1989 *J. Polym. Sci.* B **27** 753
[33] Koike T and Tanaka R 1991 *J. Appl. Polym. Sci.* **42** 1333
[34] Pochan J M, Gruber R J and Pochan D F 1981 *J. Polym. Sci. Polym. Phys. Edn.* **19** 143
[35] Koike T 1993 *Polym. Eng. Sci.* **33** 1301
[36] Johnson J F and Cole R H 1951 *J. Am. Chem. Soc.* **73** 4536
[37] Hill N E, Vaughan W E, Price A H and Davies M 1969 *Dielectric Properties and Molecular Behaviour, Van Nostrand* (London: Reinhold)
[38] Macdonald J R 1987 *Impedance Spectroscopy* (New York: Wiley)
[39] Donth E, Schröter K and Kahle S 1999 *Phys. Rev.* E **60** 1099
Reply: Arbe A, Colmenero J, Gómez D, Richter D and Farago B 1999 *Phys. Rev.* E **60** 1103
[40] Williams G 1979 *Adv. Polym. Sci.* **33** 60
[41] Kudlik A, Benkhof S, Blochowicz T, Tschirwitz C and Rössler E 1999 *J. Mol. Struct.* **479** 201
[42] Fioretto D 1999 private communication
[43] Havriliak S Jr and Havriliak S J 1994 *J. Non-Cryst. Solids* **172–174** 297
[44] Kudlik A, Tschirwitz C, Benkhof S, Blochowicz T and Rössler E 1997 *Europhys. Lett.* **40** 649
[45] Barut G, Pissis P, Pelster R and Nimtz G 1998 *Phys. Rev. Lett.* **80** 3543
[46] Hofmann A, Alegría A, Colmenero J, Willner L, Buscaglia E and Hadjichristidis N 1996 *Macromolecules* **29** 129
[47] Stickel F, Fischer E W and Richert R 1995 *J. Chem. Phys.* **102** 6251

[48] Diezemann G, Mohanty U and Oppenheim I 1999 *Phys. Rev.* E **59** 2067
[49] Schulz M 1999 *Phys. Lett.* A **251** 269
[50] Johari G P 1973 *J. Chem. Phys.* **58** 1766
[51] Corezzi S, Campani E, Capaccioli S, Fioretto D and Rolla P A 1999 *J. Chem. Phys.* **11** at press
[52] Fujara F, Geil B, Sillescu H and Fleischer G 1992 *Z. Phys.* B **88** 195
[53] Voronel A, Veliyulin E, Machavariani V Sh, Kisliuk A and Quitmann D 1998 *Phys. Rev. Lett.* **80** 2630
[54] Richter D, Zorn R, Farago B, Frick B and Fetters L J 1992 *Phys. Rev. Lett.* **68** 71
[55] Sillescu H and Bartsch E 1994 *Disorder Effects on Relaxational Processes* ed Richert and Blumen (Berlin: Springer) pp 55–88
[56] Stillinger F H 1988 *J. Chem. Phys.* **89** 6461
[57] Hodgdon J A and Stillinger F H 1993 *Phys. Rev.* E **48** 207
[58] Stillinger F H and Hodgdon J A 1994 *Phys. Rev.* E **50** 2064
[59] Kivelson S A, Zhao X, Kivelson D, Fischer T M and Knobler C M 1994 *J. Chem. Phys.* **101** 2391
[60] Tarjus G and Kivelson D 1995 *J. Chem. Phys.* **103** 3071
[61] Cohen M H and Turnbull D 1959 *J. Chem. Phys.* **31** 1164
[62] Turnbull D and Cohen M H 1961 *J. Chem. Phys.* **34** 120
[63] Turnbull D and Cohen M H 1970 *J. Chem. Phys.* **52** 3038
[64] Zwanzig R and Harrison A K 1985 *J. Chem. Phys.* **83** 5861
[65] The failure of a single VF law to reproduce the behaviour of τ over the whole temperature range above T_g was implied in the temperature behaviour of σ observed in figure 6, together with the DSE and FDSE coupling between σ and τ shown in figure 9(b). In fact, from equation (4), as well as from equation (5), it follows that if σ has a VF temperature behaviour, then also the corresponding τ has a VF behaviour with the same divergence temperature T_0.
[66] Sokolov A P 1997 *Endeavour* **21** 109
[67] Li G, Du W M, Sakai A and Cummins H Z 1992 *Phys. Rev.* A **46** 3343
[68] Donth E 1993 *Phys. Scr.* T **49** 223
[69] Schönhals A 1996 *Non Equilibrium Phenomena in Supercooled Fluids, Glasses and Amorphous Materials* ed M Giordano, D Leporini and M Tosi (Singapore: World Scientific) pp 210–14
[70] McCrum N G, Read B E and Williams G 1967 *Anelastic and Dielectric Effects in Polymeric Solids* (New York: Wiley)
[71] Baur M E and Stockmayer W H 1965 *J. Chem. Phys.* **43** 4319
[72] Hedvig P 1977 *Dielectric Spectroscopy of Polymers* (Bristol: Hilger)
[73] Yamamoto K and Namikawa H 1988 *Japan. J. Appl. Phys.* **27** 1845
[74] Yamamoto K and Namikawa H 1989 *Japan. J. Appl. Phys.* **28** 2523
[75] Yamamoto K and Namikawa H 1992 *Japan. J. Appl. Phys.* **31** 3619
[76] Huwe A, Arndt M, Kremer F, Haggenmüller C and Behrens P 1997 *J. Chem. Phys.* **107** 9699
[77] Pelster R and Simon U 1999 *Colloid Polym. Sci.* **277** 2